LAI retrieval from multi-angle and hyperspectral observations in an intensively-managed poplar plantation

M. Meroni[1,3], R. Colombo[2], M. Boschetti[1], C. Panigada[2], M. Rossini[2], P.A. Brivio[1], J.R. Miller[4]

[1] CNR-IREA, Institute for Electromagnetic Sensing of the Environment, Via Bassini 15, 20133 Milan, Italy

[2] UNIMIB-DISAT, Department of Environmental Sciences, University of Milano-Bicocca, Piazza della Scienza 1, 20126 Milan, Italy

[3] UNITUS-DISAFRI, Forest Ecology Lab, University of Tuscia, V. De Lellis s.n.c, 01100 Viterbo, Italy

[4] Department of Physics and Astronomy, York University, 4700 Keele St., Toronto M3J1P3, Canada

Abstract. LAI is retrieved from directional and hyperspectral observations by numerical inversion of coupled leaf and canopy radiative transfer models. In this research the inversion method is applied to airborne hyperspectral and multi-view-angle DAIS data (Digital Airborne Imaging Spectrometer) acquired over an intensively-managed poplar plantation. The effects of LAI and leaf Mean Tilt Angle (MTA) interactions are discussed and the magnitude of the error in LAI estimation associated with fixing the MTA to its mean value is provided by an uncertainty analysis of the inversion method. The effects of the background spectral signature are discussed and a technique for background assignment is proposed. Inversion method results are assessed comparing LAI estimates with field measurements and compared to VI-based semi-empirical regression model results.

1 Introduction

Vegetation plays a major role in land surface ecosystem functioning and Leaf Area Index (LAI) is a key biophysical parameter that describes synthetically vegetation development and vigour. LAI is required, as a driving variable in many models that estimate the water and carbon exchanges between vegetated ecosystems and the atmosphere, i.e. SVAT schemes (Soil Vegetation Atmosphere Transfer), and BGC simulation models (BioGeochemical Cycle). The knowledge of the temporal and spatial variability of this parameter is of great interest for the application of such models. RS (Remote Sensing) might provide an accurate estimate of LAI, repeatable, and spatially distributed.

The properties of vegetated surfaces are usually estimated from remote observations through semi-empirical regression models (e.g. Dawson, 2000). Such models use statistical relationships in which a limited number of *in situ* measurements of the biophysical parameter examined are usually correlated with a spectral vegetation index (e.g. Rondeaux, 1995). The robustness of these relationships is influenced by many factors: the contribution of background reflectance, the structural and biochemical canopy characteristics (foliage elements orientation and aggregation, branch contributions, vegetation vertical stratification, the spatial variability of leaf chlorophyll and water content), and finally the viewing geometry.

An alternative to the semi-empirical approach is offered by the use of radiative transfer models, which simulate the interactions of solar radiation with the vegetated medium, reconstructing the reflectivity both at leaf and canopy levels.

The use of such models in inverse mode consists of numerically minimizing the difference between remote observations and the spectral reflectances modelled for a set of biophysical parameters of interest. This technique allows the estimation of both biochemical and structural parameters in predictive mode, without requiring parameterisation (Bicheron and Leroy, 1999; Jacquemoud, 1993).

The capability to acquire nearly contemporary observations with different view angles, offered by airborne sensors and new generation satellite sensors (e.g. MISR, CHRIS-PROBA), is expected to improve the accuracy of vegetation structural parameter estimation (Verstraete and Pinty, 2001). In fact, given that the interaction of the radiation with the physical medium generates an anisotropic field of reflectivity, it is possible to describe the vegetation parameters that control this interaction (e.g. LAI) from the variation of reflectivity observed at different view angles.

2 Study area

The experiment was conducted in an intensively-managed poplar plantation located in an area periodically subjected to flooding, with variable hydrological conditions, reflecting cut-off meanders, and causing differences in standing biomass within even-aged plantations.

[Figure 1]

The study area (figure 1) is located North-East of the city of Pavia on the west bank of the Ticino river and it's representative of an intensive poplar plantation (I-214 clones, spacing 6 x 6 m) of about 120 ha. The plantation, composed by different stands with tree age ranging from two to ten years, is a permanent experimental site of CARBOEUROFLUX net managed by IES-JRC (Ispra, Italy).

3 Data collection

3.1 Field measurements

An intensive field campaign was conducted for measuring a set of parameters that are summarized in table 1.

[Table 1]

Overstory LAI and mean tilt angle (LAI_o, MTA) were estimated with Li-Cor LAI2000-PCA. Due to the relatively small area of the poplar stands the analysis of gap fractions was limited to four rings (Li-Cor, 1992). Such indirect measurements supply, more properly, an estimate of an effective LAI of the overstory (ePAI, effective plant area index, including stems and branches).

Neglecting the effects of the non-random distribution of the foliage (with clumping index Ω close to 1 in broadleaf canopy), the only correction applied was to remove the contribution of stems and branches by repeating the measurements in winter-time (no foliage present), thus measuring a stem area index (SAI), and then subtracting this value (SAI) from ePAI. This corrected estimate, $egLAI_o$ (effective green LAI of the overstory), will be referred to as $gLAI_o$ in of the remainder of this paper.

3.2 RS data

On 20/06/01, from 10.30 to 11 a.m. (local solar time), 4 and 3 stripes were acquired by DAIS (*Digital Airborne Imaging Spectrometer*) and ROSIS (*Reflective Optics System Imaging Spectrometer*) sensors (DLR-Germany), respectively. Geometric parameters of the data take and spectral characteristics of the sensors are reported in table 2 and figure 2. Flight-lines (figure 3) were designed with the aim of maximizing the number of DAIS directional observations (in the principal solar plane) of the target area.

[Table 2]

[Figure 2]

Three parallel stripes along the orthogonal solar plane and one along the principal solar plane were acquired.

[Figure 3]

Processed RS data were provided by DLR using ATCOR4 (Richter, 2000) at the correction level 2b. The atmospheric correction (based on MODTRAN4 code, Berk *et al.*, 1989) considered the effects of angular dependence of the atmospheric radiance and transmittance, and the aerosol contributions (estimated through ground photometric measurements collected during the overpass).

4 Inversion of radiative transfer models

Radiative transfer models used in this work are the canopy reflectance model SAILH (Verhoef, 1984, modified after Kuusk, 1991) and the leaf optical properties model PROSPECT (Jacquemoud and Baret, 1990).

4.1 Definition of inversion strategy and minimization algorithm

PROSPECT and SAILH model coupled (PROSAILH in the following) were inverted on hyperspectral and directional DAIS data. Spectral reflectance was averaged over a spatial window of 3x3 pixels in order to remove canopy cover discontinuities. All the available directional observations for every pixel (ranging from 2 to 4) were used simultaneously in the inversion process. Among the set of the parameters, two were fixed to a nominal value: N, the leaf structure parameter (PROSPECT) and MTA (SAILH). The N nominal value was set to 1.33 as estimated by PROSPECT inversion on leaf reflectance and transmittance spectra (Meroni *et al.*, 2002). MTA was set to its measured mean value (for a discussion on the error committed see the paragraph 4.3, Effect of LAI and MTA interaction).

The spectral domain of the merit function was selected from the available DAIS bands. Some bands were discarded due to noise and the spectral domain selected was: 808-923nm $\cup$ 1020-1033nm $\cup$ 1541-1639nm $\cup$ 1995-2291nm. In the inversion process the merit function (Δ^2) was defined as follows:

$$\Delta^2 = \Sigma_{do}\Sigma_{\lambda} [R_{obs}(VA,\lambda) - R_{mod}(VA,\lambda,P)]^2 \qquad (1)$$

where,

- Σ_{do} refers to the summation over the available directional observations;
- Σ_{λ} refers to the summation over the wavelengths of the merit function spectral domain;
- $R_{obs}(VA,\lambda)$ is the observed reflectance for a given view angle (VA) and wavelength (λ);
- $R_{mod}(P)$ is the modelled reflectance for a given view angle, wavelength and set of model parameter (P).

A quasi-Newton algorithm (NAG library, routine E04YAF) was used to minimize the merit function.

4.2 Effect of the background spectral signature

Part the poplar canopy present in the study area is characterised by a layer of understory vegetation that varies in species composition and density as a function of ecological conditions at ground level (soil type and humidity, radiation, time since the last tillage, etc.). In order to study the effect of this vegetated understory, two test areas (24m x 24m each, table 3) were selected with different forest structural conditions, and tilled few days before the overpass to completely remove the understory.

[Table 3]

The effect of the background is shown by two radiometric transects, test areas A and B, collected over the tilled areas and the nearby non-tilled areas (figure 4): along each profile the $gLAI_o$ is constant (as well as other general ecological conditions of the canopy) and thus the source of variation in canopy reflectance is due to the influences of different backgrounds (bare soil for the tilled area and understory vegetation for the untilled).

[Figure 4]

The transition from the tilled to untilled areas causes the reflectance to increase at 810 nm and to decrease at 1573 and 2122 nm because the reflectance of a vegetated background is higher than the reflectance of a bare soil in the NIR plateau and lower in the MIR wavelengths (the difference in NIR reflectance is limited in this case because the dry soil present displayed a high reflectance in this region).

This “understory effect” was also found when inverting PROSAILH on those reflectances resulting from a mixture of canopy and underlying understory, yielding an overestimation of $gLAI_o$ when a soil spectral signature was provided to the model as the background signature.

Providing the inversion with the proper background signature (collected in-field with a spectroradiometer, ASD-FieldSpec Pro) resulted in more accurate $gLAI_o$ estimation in all sites where a field spectrum was available. A further analysis of the dataset ($gLAI_o$, field spectra and inversion estimates) showed that the LAI retrieval procedure accuracy is not compromised if only the type of background signature provided in terms of broad categories: bare soil, sparse understory vegetation and dense understory vegetation (see paragraph 5, Inversion results).

In order to automatically extract this information (type of background) from RS images a neural network (NN) approach (e.g. Binaghi *et al*., 2000) was used to produce a map of the background. NN is able to integrate the contextual information of a high geometric resolution panchromatic image generated from ROSIS data with the spectral information of a selection of lower geometric resolution hyperspectral bands from DAIS (figure 5).

[Figure 5]

Below the canopy crowns, different micro-climatic conditions (radiance, moisture, and wind regime; soil type, etc.) determine the presence of diverse vegetated understory. These local conditions influence, and are partially controlled by, the structural characteristics of forest stands such as canopy closure, crown radius, trees density, etc.

The use of ROSIS high-resolution imagery (1 m pixel size) allowed taking into account these forest characteristics; whereas the hyperspectral information provided by DAIS sensor allowed the recognition of the vegetated understory presence and vigour (in terms of density classes).

4.3 Effect of LAI and MTA interaction

The analysis of a preliminary set of inversions (data not shown) evidenced that LAI and MTA were not easily separable. Even if the hot spot parameter (*sl*) is not totally independent from LAI and MTA as well (Jacquemoud *et al.*, 1995), this seems to be a minor problem when a set of directional observations is available.

A possible solution to the LAI-MTA interaction problem is to estimate separately the parameters of interest introducing constraints such as the knowledge of one parameter (Jacquemoud, 1993). An uncertainty analysis was performed in order to quantify the magnitude of the error in LAI retrieval introduced by fixing, in the inversion process, the MTA to its field mean value calculated from LAI2000 measurements.

The goal is to provide information concerning the effect of fixing MTA (an ellipsoidal leaf angle distribution was used in the model) on the accuracy of LAI estimation by generating a set of canopy spectral signature using the model in direct mode with variable input parameters (including MTA) for

3 levels of LAI (representing the range measured in field LAI=1,2,3 m^2m^{-2}) and afterward inverting the model with a fixed MTA on the generated set of spectra.

The uncertainty analysis was performed using SimLab (SimLab 1.1, 2001), software capable of global quantitative analysis, designed for Monte Carlo analysis.

The selection of ranges and distributions of input factors for Monte Carlo execution was based on the analysis of the field measurement dataset, literature, design of the inversion procedure, design of the airborne overflight (for sun and view angles). The sample set (50 arrays of input factors) was created with a stratified sampling method (*latin hypercube* sampling) in order to achieve a better coverage of the sample space of the input factors. Each element of the sample set created is supplied to the PROSAILH as input, and the model is run in direct mode 50 times for each level of LAI value considered. The results of each model evaluation are used as input in the inversion of PROSAILH: two input parameters, N and MTA, are assigned to their mean value, while the remaining is kept free. LAI estimated by inversion is the model outcome that is used for uncertainty study.

Even if significant errors arise from the largest LAI value considered, an analysis of the error in LAI estimation as a function of the deviation of the assigned MTA from the true MTA (figure 6) reveals that, in the range of one SD of the measured MTA the error is limited (table 4).

[Figure 6]

[Table 4]

5 Inversion results

Our results show that, supplying a plausible background signature to the inversion, PROSAILH provides an accurate estimation of the green LAI of the overstory ($gLAI_o$). The accuracy of the estimates was evaluated in terms of SDEP (Standard Deviation Error in Prediction) calculated on the basis of all the available LAI field measurements in the test area (n=35). Different strategies were explored in order to assign a background spectral signature to each inversion (table 5).

[Table 5]

The accuracy of each strategy (ordered on the X axis by increasing elaboration and sampling cost) is reported in figure 7 together with a description of the available dataset of LAI field measurements.

[Figure 7]

It is worth noting that the "exact" strategy is an abstraction representing the best accuracy obtainable with such approach and that it's not operatively applicable (all the background types were assigned according to the in-field inspection).
Nevertheless, the accuracy provided by the other strategies seems reasonable for most of the environmental applications (e.g. SVAT and BCG modelling).

6 A comparison with semi-empirical regression models

A number of studies demonstrated that it is possible to obtain LAI estimations through statistical regressions based on optical vegetation indices (VIs) obtained from remote sensing data of various kinds (Franklin, 1986; Spanner et al., 1990; Fassnacht et al., 1997). These relationships are formalized in different analytical expressions with coefficients largely conditioned by the type of vegetation examined and by the local environmental conditions (Chen et al., 1997; Turner et al., 1999). Among all the proposed LAI-VIs relationships we will refer to the widely-used LAI-NDVI regression model.

A comparison of the performances of PROSAILH and semi-empirical LAI-NDVI regression models in estimating the overstory green LAI is rather difficult. These approaches are different in "nature": PROSAILH being predictive (no *in situ* calibration is needed) while regression models need for calibration by definition. Moreover, NDVI is related to the total green LAI (overstory+understory) whereas PROSAILH seems able to isolate the overstory contribution when a plausible background spectral signature is provided.

Regression estimations should be accurate when the proportion between overstory green LAI and total green LAI of the samples used in calibration is of the same magnitude as that included in the samples on which the regression is applied in prediction. Further it is necessary that the variance of the factors

(other than LAI) controlling the spectral response of the canopy (e.g. soil reflectance, leaf biochemistry) is fully accounted for in the calibration set.

PROSAILH estimates, on the other hand, should be reliable when the hypotheses of the model are met, i.e. the canopy can be represented by a turbid medium. Assuming that the model hypotheses are satisfied, that a single regression may be used to estimate LAI in the study area, and that measurements are not affected by random errors, the following exercise was designed in order to compare the accuracies (SDEP) of PROSAILH and a typical LAI-NDVI regression model (DAIS data from flightline in the principal solar plane were used). SDEP was calculated as follows: the set of available LAI field measurements (n = 35) was divided in two subsets: one for the regression coefficients computation (70% of the measurements) and the other one to test the regression (SDEP computation). Then, in order to simulate a number of possible *in situ* LAI planning scheme strategies, 21 arrays of k samples (with k ranging form 4 to the total number of available measurements, 25) were extracted from the first subset. Each array of this set was then used to calibrate the regression (a logarithmic relationship between NDVI and $gLAI_o$, showing the highest coefficient of determination, was used). The SDEP of the regression was then calculated on the testing set. The process was repeated 50 times to explore the variability of the accuracy as a function of the particular sample chosen.

Each sample extraction (including the testing set) was performed by a stratified sampling method in which the samples were chosen randomly ensuring the coverage of the sample full range, simulating the condition of a priori knowledge of LAI variability that is not always achievable in field. The results of this exercise are shown in figure 8.

[Figure 8]

Regressions show a large SDEP variation when they are calibrated using a limited sample number. This is due to the proportion of green LAI overstory/green LAI not included in the calibration set dynamically considered, together with the soil reflectance and leaf biochemistry variability, etc. Such calibration sample set may indeed be, or not be, representative of the variability present in the testing set. When the number of sample used in regression calculations is increased, a lower SDEP variation

is observed, indicating that regression predictions are insensitive to the composition of the particular sample used.

The magnitude of the reduction in SDEP variation for increasing number of sample (note that is obviously 0 when all 25 samples are used) represents a trend that cannot be generalized because the population variance (the total variance) might not be fully explained by the presented sample variance. Thus, a safe threshold on the number of measurements to be taken in field cannot be deduced.

6 Conclusion

In this work, coupled PROSPECT and SAILH models were inverted to estimate the leaf area index with an acceptable accuracy. Some strategies for minimizing the effect of a rather varying understory were tested: the availability of a background map seems crucial to the LAI retrieval accuracy.

The NN understory map (paragraph 4.2) fails to recognize the correct background when the overlaying canopy cover is dense. This occurrence does not diminish the map's utility because in such a situation (dense canopy) the understory influence on model inversion is minimal. The analysis of LAI estimation error confirms this hypothesis: $gLAI_o$ estimation SDEP is contained even in correspondence with map error in understory assignment.

A comparison exercise between regression models and inversion of PROSAILH model showed that regressions calibrated with a limited number of LAI-NDVI pairs provide an accuracy that is highly variable depending on the particular sample chosen.

PROSAILH estimate accuracy is comparable with that of regression models (higher when a map of the background type is used in the selection of the background reflectance to be provided to the inversion algorithm).

Acknowledgements

DAIS and ROSIS data were provided by DLR-Germany in the framework of the EU-funded HySens project. The authors gratefully acknowledge G. Seufert and the Climate Change unit staff (JRC-IES, Ispra), S. Jacquemoud, C. Bacour (LED - Université Paris 7), S. Tarantola (IPSC-JRC, Ispra, Italy), for their contributions and suggestions.

The understory map analysis is current research conducted by I. Gallo (CNR-ITBA, Italy) and E. Binaghi (University of Insubria, Italy) in collaboration with remote sensing department of IREA-CNR.

References

BERK, A., BERNSTEIN, L.S., ROBERTSON, D., 1989, Modtran: A moderate resolution model for Lowtran 7. GL-TR-89-0122, Geophysical Laboratory, Bedford, MA.

BICHERON, P., LEROY, M., 1999, A method of biophysical parameter retrieval at global scale by inversion of a vegetation reflectance model, Remote Sensing of Environment, 67, 251-266.

BINAGHI**,** E**.,** BRIVIO**,** P.A**.,** GALLO, I., PEPE, M., RAMPINI, M., 2000, Soft computing techniques for high accuracy Remote Sensing data classification. In Recent Developments in Pattern Recognition Research, edited by B. Chandrasekaran, M.D. Levine, C.H. Chen (Transworld Research Network Publishing), pp. 89-112.

CHEN, J. M., RICH, P. M., GOWER, S. T., NORMAN, J. M., PLUMMER, S., 1997, Leaf Area Index of Boreal Forests: Theory, techniques, and measurements, Journal of Geophysical Research, BOREAS Special Issue, 102, 29429-29443.

DAWSON, T.P., 2000, The potential for estimating chlorophyll content from a vegetation canopy using MERIS, International Journal of Remote Sensing, 21, 2043–2051

FASSNACHT, K.S., GOWER, S.T., MACKENZIE, M.D., NORDHEIM, E.V., and LILLESAND, T.M., 1997, Estimating the Leaf Area Index of north central Wisconsin forest using the Landsat Thematic Mapper, Remote Sensing of Environment, 61, 229-245.

FRANKIN, J., 1986, Thematic mapper analysis of coniferous forest structure and composition, International Journal of Remote Sensing, 10, 1287-1301.

JACQUEMOUD, S., BARET, F., 1990, PROSPECT: a model of leaf optical properties spectra, Remote Sensing of Environment, 34, 75–91.

JACQUEMOUD, S., 1993, Inversion of the PROSPECT + SAILH canopy reflectance model from AVIRIS equivalent spectra: Theoretical study, Remote Sensing of Environment, 44, 281 – 292.

JACQUEMOUD, S., BARET, F., ANDRIEU, B., DANSON, F.M., JAGGARD, K., 1995, Extraction of Vegetation Biophysical parameters by Inversion of the PROSPECT + SAILH Models on Sugar Beet Canopy Reflectance Data. Application to TM and AVIRIS Sensors, Remote Sensing of Environment, 52, 163–172.

KUUSK, A., 1991, The hot-spot effect in plant canopy reflectance, in Photon-vegetation interactions; Application in optical remote sensing and plant ecology, edited by R. Myneni and J. Ross (Springer-Verlag, New York), 139 – 159.

LI-COR, 1992, LAI-2000 plant canopy analyzer instruction manual, LI-COR, Inc., Lincoln, Nebraska

MERONI, M., PANIGADA, C., COLOMBO, R., BOSCHETTI, M., BRIVIO, P.A., MARINO, C.M., 2002, Osservazioni remote iperspettrali e multiangolari per la stima dei parametri biofisici della vegetazione: parte II – tecniche di telerilevamento, Rivista Italiana di Telerilevamento, in press.

RICHTER, R., 2000, ATCOR4 user manual, DLR-IB 564-04/2000.

RONDEAUX, G., 1995, Vegetation monitoring by remote sensing: a review of biophysical indices, Photo-Interpretation, 3, 197–216.

SIMLAB 1.1 Version 1.1 Reference Manual, 2001, POLIS ISIS-JRC.

SPANNER, M.A., PIERCE, L.L,. PETERSON, D.L., and RUNNING, S.W., 1990, Remote sensing of temperate coniferous forest leaf area index. The influence of canopy closure, understory vegetation and background reflectance, International Journal of Remote Sensing, 11, 95-111.

TURNER, D.P., COHEN, W.B., KENNEDY, R.E., FASSNACHT, K.S., BRIGGS J.M., 1999, Relationship between Leaf Area Index and Landsat TM Spectral Vegetation Indices across three temperate zone sites, Remote Sensing of Environment, 70, 52 - 68.

VERHOEF, W., 1984, Light scattering by leaf layers with application to canopy reflectance modeling: the SAILH model, Remote Sensing of Environment, 16, 125 – 141.

VERSTRAETE, M.M., PINTY, B., 2001, Introduction to special section: Modeling, measurement, and exploitation of anisotropy in the radiation field, Journal of Geophysical Research, 106(11),

903–907.

FIGURES:

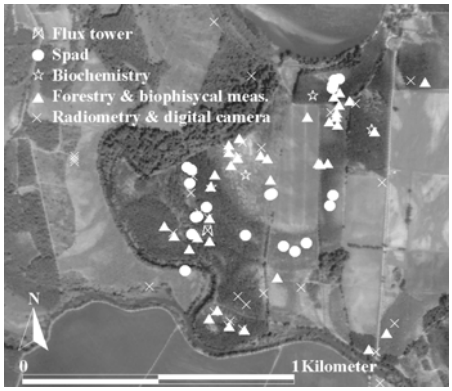

Figure 1: Study area and field measurements (see table 1).

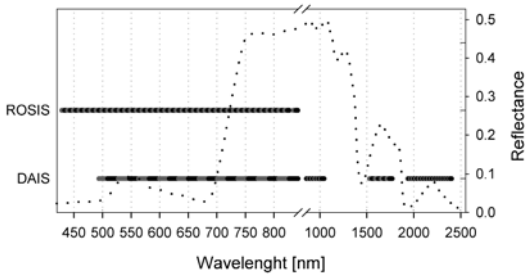

Figure 2: Position and width of DAIS and ROSIS bands.

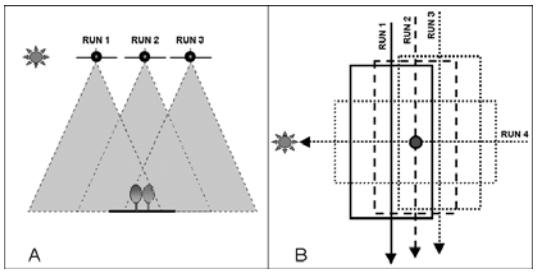

Figure 3: Flightlines geometry, front view (A), ground projection (B).

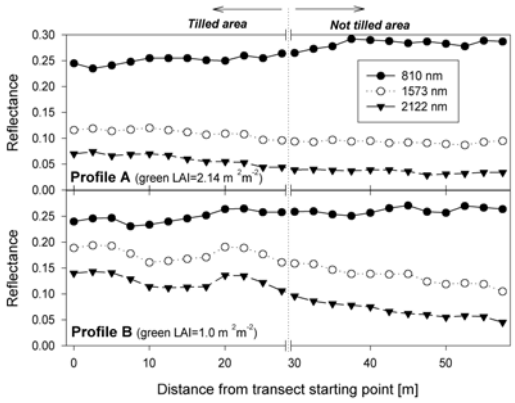

Figure 4: Radiometric transects referring to A and B test areas: the starting point is located in the tilled area, after distance 30m the reflectance refers to a canopy over a non-tilled terrain. Wavelengths are reported in the graphic.

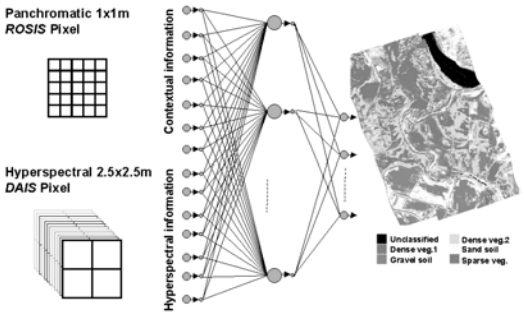

Figure 5: Extraction of the background map using high geometric and high spectral resolution data and NN.

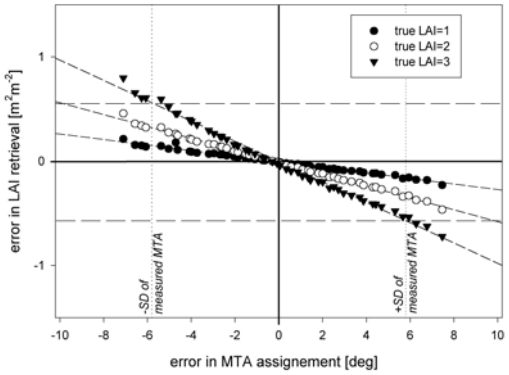

Figure 6: Error in LAI prediction as a function of the error committed in fixing the MTA in the inversion process (error in MTA ass. = ass. MTA – true MTA; error in LAI retr. = retr. LAI – true LAI).

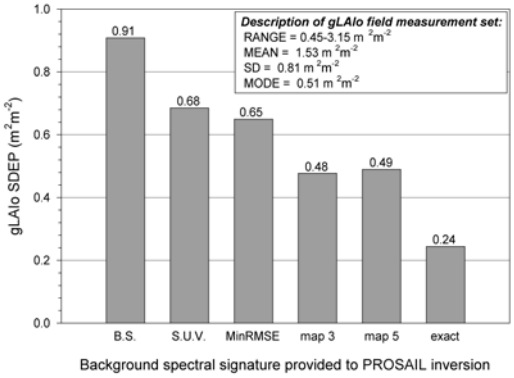

Figure 7: PROSAILH inversion $gLAI_o$ SDEP for different background spectral signature assignment (for the acronyms see Table 4).

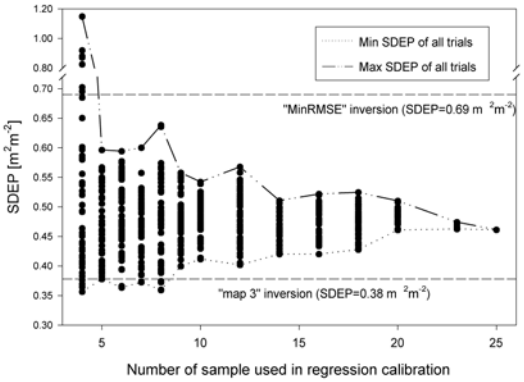

Figure 8: SDEP of regression models (as a function of the number of sample used in calibration), and of PROSAILH model inversions of MVA data, calculated on the same dataset (10 test samples).

TABLES:

Category	Parameters	Technique
Forestry		
	Tree diameter and height, crown radius	Direct measurements
Radiometry		
	Aerosol optical thickness[1], leaf reflectance and transmittance[2], spectra of surfaces[3]	[1]Photometer, [2]spectrorad., [3]spectrorad. + integ. sphere
Biophysical parameters		
	MTA_o[1], LAI_t (total)[1], LAI_o[1], LAI_u[1]; fractional cover: Fc_o[1,2], Fc_u[2,3]	[1]Li-Cor LAI2000, [2]direct meas., [3]digital camera
Biochemical parameters		
	Leaf relative chlorophyll content[1], Leaf chlorophyll ab[2], Leaf water[2], SLA[2] (Specific Leaf Area)	[1]Minolta Spad 502, [2]laboratory measurements

Table 1: Field measurements summary. Subscripts *o* and *u* refer to overstory and understory, respectively and superscript number link parameter with measurement technique.

Sensor	Altitude	Swath, FOV	pixel size
DAIS	1800 m	1280 m, ±29°	250×250 cm
ROSIS	1800 m	420 m, ± 8°	100×100 cm

Table 2: Data take geometric characteristics.

Test area	LAI_o	$gLAI_o$	Fc%
A	2.33	2.14	90
B	1.5	1	60

Table 3: Structural characteristics of the test areas selected, Fc is the canopy crowns fractional cover.

	LAI=1	LAI=2	LAI=3
SDEP	0.08	0.17	0.30
Mean	0.99	1.99	2.99
SD	0.08	0.17	0.30

Table 4: Standard Deviation Error in LAI Prediction (SDEP) caused by fixing the MTA; mean and standard deviation of the predicted values in one SD of the measured MTA are reported for the three levels of LAI considered.

	Method
B.S.	Spectral signature of Bare Soil was provided to every inversion
S.U.V.	Spectral signature of a Sparse Vegetated Understory provided to every inversion
MinRMSE	Each inversion was repeated with three possible backgrounds (bare soil, sparse understory, dense understory), the estimate showing the minimum RMSE in the minimization process was chosen
map 5	The background map (paragraph 4.2), was used as a criterion to assign the background signature
map 3	As in map 5, the background map was resampled to 3 classes (see MinRMSE)
exact	The most appropriate background for each inversion was supplied

Table 5: Summary of background assignment strategies.